Nanoscale Advances

COMMUNICATION

Cite this: *Nanoscale Adv.*, 2019, **1**, 481

Received 19th June 2018
Accepted 7th October 2018

DOI: 10.1039/c8na00051d

rsc.li/nanoscale-advances

Sunlight active U_3O_8@ZnO nanocomposite superfast photocatalyst: synthesis, characterization and application†

K. Raagulan,[ab] M. M. M. G. P. G. Mantilaka,[*ac] G. T. D. Chandrakumara,[c] U. G. Mihiri Ekanayake,[ac] W. P. S. L. Wijesinghe,[ac] Shanmuganathan Ehanathan,[a] R. M. G. Rajapakse,[ad] Ramanaskanda Braveenth[b] and Kyu Yun Chai[*b]

Sunlight active U_3O_8@ZnO nanocomposite photocatalyst has been synthesized for the first time using co-precipitation method. The synthesized composite has a particle size ranging from 18 nm to 30 nm with band gap energy of 2.9 eV. The composite photocatalyst is capable of degrading methylene blue completely within 30 min under sunlight irradiation. Therefore, this superfast efficient sunlight-active photocatalyst is very useful in industrial organic waste water treatment.

Large number of industries including textile, petroleum, cosmetics, paper, leather, pharmaceutical, rubber, plastic, pesticides and food consume enormous quantities of organic chemicals as raw materials and consequently excessive amounts of these chemicals are released into water bodies as waste effluents.[1] Hence, various techniques have been developed for water purification with various chemical, physical and biological methods including coagulation, flocculation, filtration, precipitation, ion exchange, membrane-filtration, adsorption techniques, biodegradation methods and catalytic routes like photocatalysis.[2] Among these techniques, photocatalysis plays a vital role because it breaks organic pollutants into simplest gaseous forms without generating secondary pollutants.

Many types of semiconductors have been studied as photocatalysts such as TiO_2, ZnO, CdS, WO_3, and so on.[1,3] Most photocatalysts are UV active; UV lights are required for efficient degradation of organic pollutants in effluents. Therefore, photocatalysts active under both UV and visible light are attractive, efficient and cost effective for industrial effluent treatment plants compared to those active only under UV as UV-vis active catalysts are useful to degrade organic pollutants under direct sunlight. In order to fulfill this requirement, band gap of photocatalyst has to be narrowed or split into several sub-band gaps, which can be achieved through non-metal/metal doping, coupling semiconductors or dye sensitization. In core–shell semiconductor nanocomposites, nanocrystals are composed of a quantum dot semiconducting core material and a shell of a distinct semiconducting material in which electrons are injected from core to the shell generating the photocurrent, which depends on exciton dissociation at the core–shell interface and relative alignment of conduction and valence-band edges of the core and shell. Furthermore, both electrons and holes are in the core region and electrons and holes are spatially separated into core and shell regions.[4–6]

In this research, U_3O_8@ZnO nanocomposite spheres with particle size 18–30 nm were formulated and synthesized for the first time by co-precipitation method as a sunlight active superfast photocatalyst. The synthesized catalyst is capable of full degradation of standard model dye, methylene blue (MB), under 30 min of sunlight irradiation. The catalyst has a bandgap energy of 2.9 eV and is active under visible light. Therefore, the synthesized material is useful in organic dye degradation under direct sunlight, which is very useful for industrial effluent treatment plants.

In the synthesis procedure of the composite photocatalyst, 100 ml of 0.1 M uranyl nitrate solution and 100 ml of 0.1 M $ZnSO_4$ solution were mixed together and stirred for 2 min. 0.2 ml of 25% CTAB was added into the mixture while stirring, until the temperature reached 80 °C. 10% (w/w) ammonia solution [$NH_4OH_{(aq)}$] was added drop-wise while the supernatant was being tested with 0.1 M sodium phosphate solution [$Na_3PO_{4(aq)}$]. Constant temperature of 80 °C was maintained while stirring for 1 h with occasional ultra-sonication. Equal volume of distilled water was added to the above solution in order to dilute the concentration by 0.5 and kept under similar

[a]*Postgraduate Institute of Science, University of Peradeniya, Peradeniya, 20400, Sri Lanka. E-mail: manthilaka@gmail.com; prasangam@slintec.lk; Tel: +94114650556*
[b]*Division of Bio Nano Chemistry, Wonkwang University, Iksan, Jeollabuk-do, South Korea. E-mail: geuyoon@wonkwang.ac.kr; Tel: +82638506230*
[c]*Sri Lanka Institute of Nanotechnology, Nanotechnology and Science Park, Mahenwatte, Pitipana, Homagama, Sri Lanka*
[d]*Department of Chemistry, Faculty of Science, University of Peradeniya, Peradeniya, 20400, Sri Lanka*

† Electronic supplementary information (ESI) available. See DOI: 10.1039/c8na00051d

conditions for 15 min. The mixture was sonicated for 20 min. Then, it was filtered and thoroughly washed with 50 ml aliquots of distilled water three times. A yellow color product was obtained and it was air-dried overnight. The product was autoclaved at 120 °C for 2 h and filtered using suction filtration. Final product was calcined at 800 °C for 2 h to obtain the U_3O_8@ZnO nanocomposite.

The crystalline phases of U_3O_8@ZnO was analyzed by X-ray diffraction (XRD) using a Siemens D5000 Powder X-ray Diffractometer (Cu Kα $\lambda = 0.1540562$ nm and scanning rate of 1° min^{-1}). XRD patterns were analyzed with the aid of the ICDD PDF 2 database. The average sizes of crystallites were estimated using the Debye–Scherrer formula, which was applied to high intensity XRD peaks.[7] Hitachi SU6600 Scanning Electron Microscope (SEM) was used to examine morphology and average size of particles with an accelerating voltage of 10 kV. Energy-dispersive X-ray (EDX) spectroscopy was used to observe the elemental distribution of the composite with a scanning rate of 192 000 CPS for 4 min. The Fourier Transform Infrared (FT-IR) spectra was recorded on a Shimadzu IR Prestige 21 instrument with the KBr pellet method. Herein, the ratio of sample to KBr was maintained at 1 : 40 and the pellets were prepared by applying 5 tons of pressure. UV-visible spectroscopy (UV-1800 Shimadzu) was used to obtain UV-vis spectrum of the composite and methylene blue solutions. High performance liquid chromatography (HPLC) studies were conducted to evaluate the degraded products of methylene blue using Waters Alliance 2695 instrument with Waters 2998 PDA detector.

Methylene blue was used as a standard model dye to evaluate photocatalytic performance of the composite. 0.001 g of U_3O_8@ZnO powder was dispersed in 250 ml of 5 ppm MB solution in a dark place. The suspended solution was stirred for 30 min and kept for 10 h in the same conditions to allow the system to come to the adsorption equilibrium in order to avoid experimental errors due to adsorption of MB on to the catalyst. The resultant equilibrated solution was then exposed to sunlight for 1 h with occasional shaking during which period 5 ml of sample was siphoned off in 5 min time intervals. The obtained 5 ml exposed samples were centrifuged at 4000 rpm for 10 min to separate MB solution from dispersed catalyst and analyzed under UV-visible spectroscopy. The efficiency of dye degradation was calculated using eqn (1) below.

$$q_0 = \frac{C_0 - C}{C_0}\% \quad (1)$$

where q_e is the efficiency of dye degradation, C_0 is the initial concentration and C is the concentration of MB after irradiation by sunlight.

The FTIR spectrum (Fig. 1a) of the synthesized product before calcination exhibits bands at 825 cm^{-1} and 943 cm^{-1} ascribed to UO_2^{2+} group; these are characteristic bands of UO_2^{2+} complexes. The C–O bonds found in FTIR bands at 1435 cm^{-1} and 1234 cm^{-1} confirm the possibility of U(VI) carbonate complex formation.[8] The most typical bond recognized in FTIR is Zn–O at the finger print region at 410 cm^{-1} (400–500 cm^{-1}).[1] So, zinc is available in the sample, which is further confirmed by elemental analysis, which is described later. The broad band

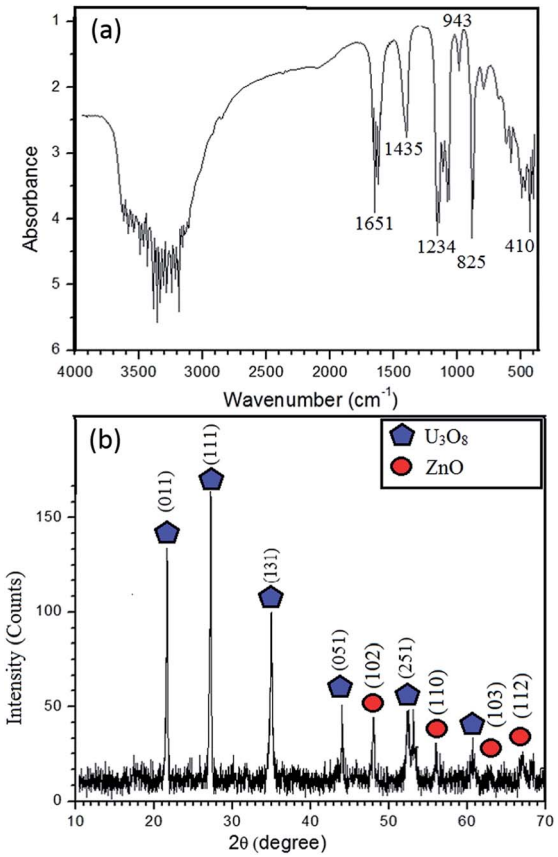

Fig. 1 (a) FT-IR spectrum of $UO_2(OH)_2$/$Zn(OH)_2$. CTAB (b) XRD pattern of the synthesized U_3O_8@ZnO nanocomposite.

between 3000 and 3500 cm^{-1} indicates the stretching mode of OH^- and 1600 cm^{-1} imply the bending mode. Further, bands at 3200 and 1651 cm^{-1} indicate the stretching vibrations of alkane from CTAB. Shoulder of the N–H stretching absorptions between 3400 and 3500 cm^{-1} indicates the primary amine, which is the terminal group of CTAB.[9] FTIR results reveal that the synthesized nanocomposite consists both Zn and U. Solubility product of $UO_2(OH)_2$ is in the order of 10^{-23}, while solubility product of $Zn(OH)_2$ is in the order of 10^{-17}.[10,11] According to the solubility, $UO_2(OH)_2$ could form core, whereas $Zn(OH)_2$ acts as shell. Hence, the un-calcined product is $UO_2(OH)_2$@-$Zn(OH)_2$ with CTAB.

XRD pattern (Fig. 1b) confirms that the synthesized material is crystalline and it is in good agreement with FTIR results. The peak positions at 2θ values of 21.65°, 27.23°, 34.98°, 43.99°, 52.413° and 60.61° can be assigned to those of orthorhombic polycrystalline U_3O_8.[12] The typical high intensity peak of U_3O_8 occurs at 27.23°, which implies that the U_3O_8 precursor has been annealed properly at 800 °C. Some of the ZnO peak positions are adjacent to those of U_3O_8, which are found to be at 2θ values of 47.54°, 56.60°, 63°, 66.37° and 69.14° and occurrence of these peaks implies formation of polycrystalline ZnO with wurtzite structure.[13] According to the Scherrer equation, the average crystallite size of U_3O_8@ZnO is approximately 27 nm.[8]

EDX results, as shown in Fig. 2, confirm the presence of Zn, U and O in the composite with atomic percentages of 20.01%,

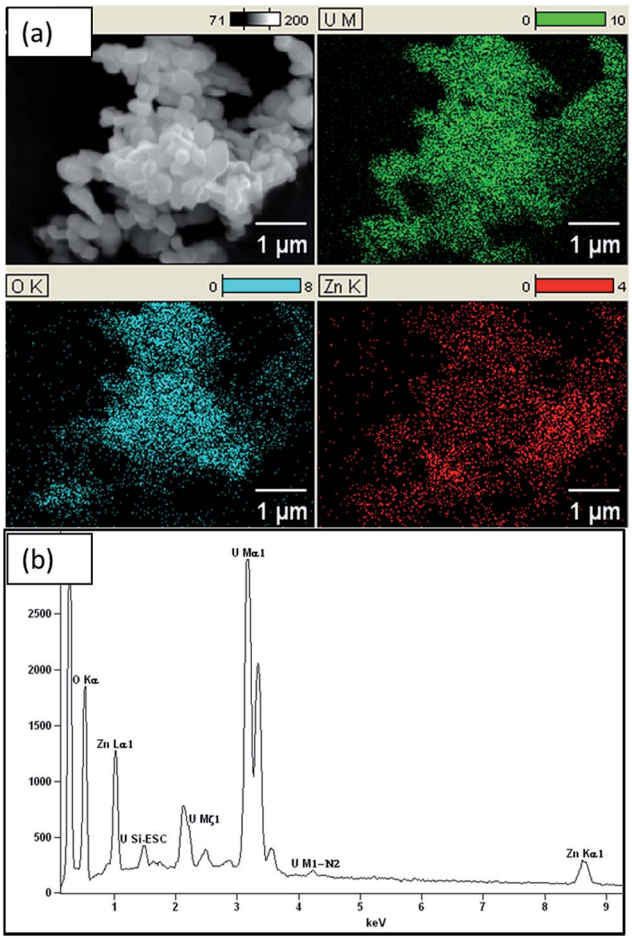

Fig. 2 EDX (a) mapping and (b) spectrum of U_3O_8@ZnO nanocomposite.

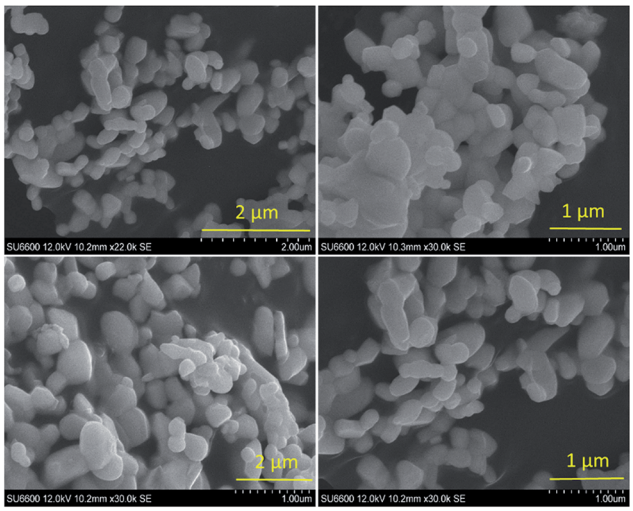

Fig. 3 SEM images of U_3O_8@ZnO nanocomposite.

19.63% and 60.37%, respectively. Thus, Zn to U atomic ratio of the composite is 1 : 1. In addition, the atomic percentage of ZnO is about 40% and remaining part is U_3O_8. Hence, ratio between Zn and O is 1 : 1, whereas U : O ratio is about 1 : 2.1. Further, Chave *et al.* reported that at 800 °C $UO_2(OH)_2$ converts into U_3O_8. Hence, formula of the composite is U_3O_8@ZnO.[14,15] EDX results confirm that the U_3O_8@ZnO has been formed as required and the ZnO amount is greater than that of U_3O_8. The SEM images (Fig. 3) depict that the morphology of U_3O_8·ZnO is spherical with particles in nanometer scale. However, these spheres have been aggregated to form various irregular formations. According to SEM study, the particle diameter is in the range 18–30 nm and aggregate particles are in micrometer range (Fig. 4).

Fig. 5 shows the UV-vis spectra of MB under different time periods of sunlight irradiation, which was degraded by the nanocomposite. The maximum visible light absorption of MB dye is found to be at 663 nm. Peak drastically reduced with the addition of the composite catalyst under sunlight. The photocatalytic degradation efficiency (q_e) of MB dye containing composite catalyst under sunlight irradiation at 5, 10, 15, 20 and 30 min are 93.04, 97.88, 96.5, 99.17 and 100% respectively. MB was fully degraded within 30 min of sunlight irradiation, which can be confirmed by the disappearance of UV-vis spectrum at this point. UV-vis study on the mixture of U_3O_8@ZnO catalyst and methylene blue solution kept under dark conditions confirms that the U_3O_8@ZnO is a photocatalyst, not an adsorbent as shown in supplementary data Fig. S3.† Fig. 6a shows the first order kinetic plot of $\ln(C_0/C)$ *versus* the irradiation time, which shows that the reaction follows first order kinetics. The rate constant (k) and the half-life ($t_{1/2}$) values of degradation reaction are 0.1038 min^{-1} and 6.68 min respectively. Fig. 6b shows photographs of dye solution with catalyst before and after irradiation by sunlight, which is visibly evident with the production of clean water with the catalyst and sunlight.

HPLC results, as shown in Fig. S1 in ESI,† reveal that the high intensity methylene blue peak disappeared in the photodegraded final solution during photocatalysis under sunlight. The HPLC of final solution contains only water as compared with HPLC results of deionized water. This means that methylene blue is fully degraded into CO_2 and H_2O by the synthesized

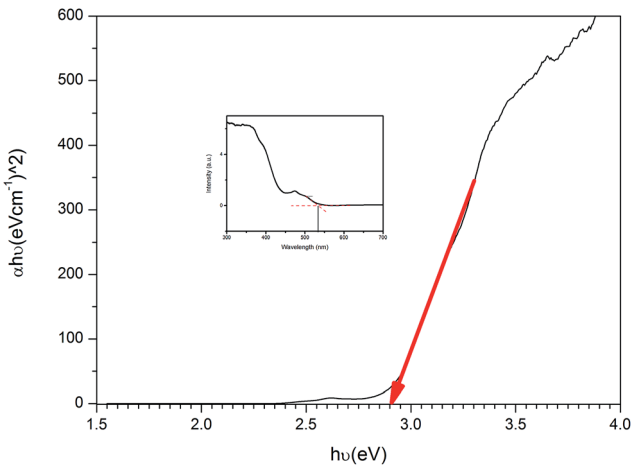

Fig. 4 Solid state UV-vis based Tauc plot of U_3O_8@ZnO nanocomposite.

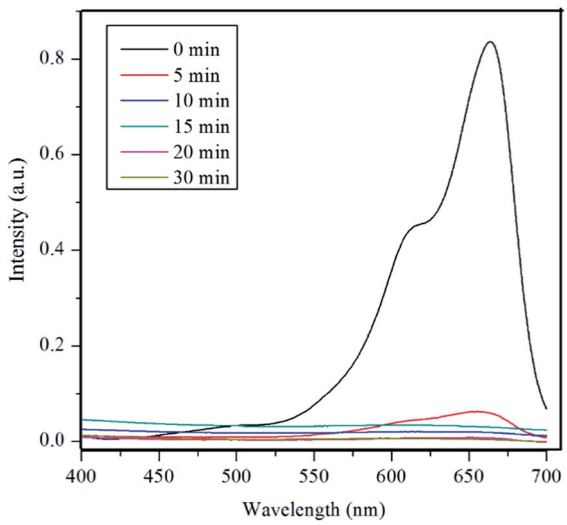

Fig. 5 UV-vis spectra of MB under different time periods of sunlight exposure with U_3O_8@ZnO nanocomposite catalyst.

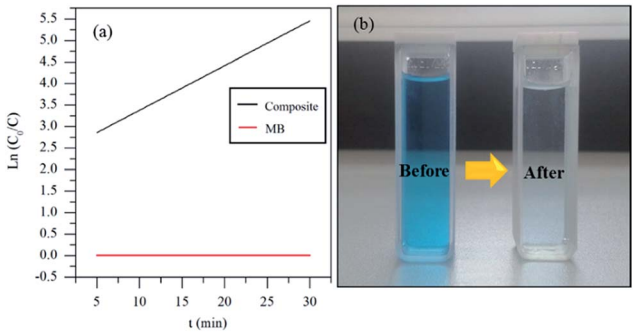

Fig. 6 (a) Degradation kinetics and (b) before and after degradation of MB by the synthesized U_3O_8@ZnO catalyst.

U_3O_8@ZnO photocatalyst under sunlight. Furthermore, the catalyst is stable after the degradation, which is confirmed by unchanged peaks of XRD pattern of the catalyst after using for degradation of methylene blue (ESI Fig. S2†).

The efficient photocatalyst accelerates the photoreaction in the presence of light energy, which is absorbed by the catalyst causing electron migration from valance band (VB) to conduction band (CB) and creation of electron–hole pairs. Photo-induced reactions occurring at the surface of the catalyst depends on the rate of formation of electron–hole pairs. Holes generated in valance band, able to accept electron due to this holes breed generates various reactive oxygen species (ROSs) like $^{\cdot}OH$, $^{\cdot}OOH$, H_2O_2 in water medium are highly oxidizing in nature. This is crucial in degradation of organic substances by loss of electron. These species are responsible for the degradation of organic contaminants and disinfection of pathogenic microorganisms. Methylene blue is a cationic dye, which can easily adsorb on to the surface of the catalyst. This is favorable for efficient charge transfer.[16]

$$\text{Semiconductors} + h\nu \rightarrow h^+_{VB} + e^-_{CB}$$

$$h^+_{VB} + H_2O \rightarrow OH^- + H^+$$

$$e^-_{CB} + O_2 \rightarrow O_2^-$$

$$R + {}^{\cdot}OH \rightarrow R^{\cdot} + H_2O$$

$$R + h^+ \rightarrow R^{\cdot +} \rightarrow \text{degradation of R}$$

According to the literature degradation rate of MB using commercial amorphous anatase TiO_2,[9] bromophenol blue dye using ZnO flower like structure(~96%, 120 min),[1] cesium doped chromium oxide thin film synthesized using spray pyrolysis,[17] graphene@TiO_2 "dyade" like structure (88% degradation for 100 min),[18] ZnO:Eu nanoparticles[19] are lower than that of U_3O_8@ZnO nanocomposite and they degrade MB under exposure to UV light only.[9] Therefore, this is a more effective photocatalyst than bare ZnO nanoparticles.

Conclusions

Crystalline U_3O_8@ZnO nanocomposite is successfully synthesized for the first time by co-precipitation with average particle size ranging from 18 nm to 30 nm. The synthesized materials is visible light active photocatalyst with bandgap of 2.9 eV. Also, 30 min irradiation of sunlight in the presence of 0.001 g of catalyst could degrade 250 ml of 5 ppm MB solution following first order kinetics. This clearly shows that the synthesized U_3O_8@ZnO material is a superfast photocatalyst. Therefore the synthesized photocatalyst is useful for industrial organic effluent treatment processes.

Conflicts of interest

There are no conflicts to declare.

Acknowledgements

Authors thank C. A. Thennakoon, R. B. S. D. Rajapakshe and Dr K. G. Chathuranga Senarathna at University of Peradeniya for their enormous support. We also acknowledge National Research Council (Grant no. 16-123), Sri Lanka for partial financial assistance.

Notes and references

1 S. Ameen, M. Shaheer Akhtar and H. Shik Shin, *Mater. Lett.*, 2017, **209**, 150–154.
2 X. Qu, P. J. J. Alvarez and Q. Li, *Water Res.*, 2013, **47**, 3931–3946.
3 N. Guo, Y. Zeng, H. Li, X. Xu and H. Yu, *Mater. Lett.*, 2017, **209**, 417–420.
4 Q. Que, Y. Xing, Z. He, Y. Yang, X. Yin and W. Que, *Mater. Lett.*, 2017, **209**, 220–223.
5 Z. Zhu, Q. Han, D. Yu, J. Sun and B. Liu, *Mater. Lett.*, 2017, **209**, 379–383.

6 Y. C. Chang, J. Y. Guo and C. M. Chen, *Mater. Lett.*, 2017, **209**, 60–63.
7 R. Wahab, Y. Kim and H. Shin, *Mater. Trans.*, 2009, **50**, 2092–2097.
8 A. Rossberg, K. U. Ulrich, S. Weiss, S. Tsushima, T. Hiemstra and A. C. Scheinost, *Environ. Sci. Technol.*, 2009, **43**, 1400–1406.
9 K. Bubacz, J. Choina, D. Dolat and A. W. Morawski, *Pol. J. Environ. Stud.*, 2010, **19**, 685–691.
10 K. Fujiwara, H. Yamana, T. Fujii, K. Kawamoto, T. Sasaki and H. Moriyama, *J. Nucl. Sci. Technol.*, 2005, **42**, 289–294.
11 R. A. Reichle, K. G. McCurdy and L. G. Hepler, *Can. J. Chem.*, 1975, **53**, 3841–3845.
12 B. O. Loopstra, *Acta Crystallogr.*, 1964, **17**, 651–654.
13 M. J. Akhtar, M. Ahamed, S. Kumar, M. M. Khan, J. Ahmad and S. A. Alrokayan, *Int. J. Nanomed.*, 2012, **7**, 845.
14 T. Chave, S. I. Nikitenko, A. C. Scheinost, C. Berthon, B. Arab-Chapelet and P. Moisy, *Inorg. Chem.*, 2010, **49**, 6381–6383.
15 L. L. Oliveira, Ana L. Dantas, S. S. Pedrosa, G. O. G. Rebouças, R. B. da Silva, J. M. de Araújo and A. S. Carriço, *Phys. Rev. B*, 2018, **97**, 134413.
16 A. Tuerdi, A. Abdukayum and P. Chen, *Mater. Lett.*, 2017, **209**, 235–239.
17 T. Larbi, M. A. Amara, B. Ouni and M. Amlouk, *Mater. Res. Bull.*, 2017, **95**, 152–162.
18 D. Zhao, G. Sheng, C. Chen and X. Wang, *Appl. Catal., B*, 2012, **111–112**, 303–308.
19 L. V. Trandafilović, D. J. Jovanović, X. Zhang, S. Ptasińska and M. D. Dramićanin, *Appl. Catal., B*, 2017, **203**, 740–752.